

Nuclear statistics of dysprosium resonance parameters in the energy range 10 – 1000 eV

S. G. Shin^a, Y. U. Kye^a, G. N. Kim^c, M. W. Lee^d, Y. R. Kang^d, W. Namkung^b, T. I. Ro^e, and M. H. Cho^{a*}
^a Department of Advanced Nuclear Engineering, POSTECH, 77 Cheongam-Ro, Nam-Gu, Pohang 37673, Korea
^b Pohang Accelerator Laboratory, 127 Jigok-Ro, Nam-Gu, Pohang 37673, Korea
^c Kyungpook National University, 80 Daehak-Ro, Buk-Gu, Daegu 41566, Korea
^d Dongnam Inst. Of Radiological & Medical Science, 40 Jwadong-Gil, Jangan-Eup, Gijang-Gun, Busan, Korea
^e Department of Physic, Dong-A University, Busan 49315, Korea
 *mhcho@postech.ac.kr

1. Introduction

A resonance parameter analysis is often performed in the Resolved Resonance Region (RRR) in order to estimate the average level spacing, distribution of the reduced widths and so on. Neutron Capture experiments on dysprosium isotopes were performed at the electron linear accelerator (LINAC) facility of the Rensselaer Polytechnic Institute (RPI) in the neutron energy region from 10 eV to 1 keV. Resonance parameters were extracted by fitting the neutron capture data using the SAMMY multilevel R-matrix Bayesian code [1].

The resonance parameters of the dysprosium isotopes have been analyzed in Reference [2, 3]. The following nuclear statistics of the resonance parameters will be discussed in this paper.

- Average level spacing,
- Porter-Thomas distribution for the reduced neutron width,
- Neutron strength function

2. Experimental Setup and Data Reduction

A detailed description of the present measurement and analysis is given in Reference [2, 3], so only a brief description is given in the present paper.

The ~57 MeV electron beam which is produced by the RPI LINAC impinges on a water-cooled tantalum target while photo-neutron reactions happen and pulsed neutrons are generated via the reactions. The details of the experimental conditions such as neutron targets overlap filters, pulse repetition rate, flight path length, and channel widths are listed on reference [2]. More information on the water-cooled tantalum target [4, 5], the capture detector [6,7], the data acquisition system [6,8], and sample information [2] were given elsewhere.

Data taking and data reduction technique for the experiment at the RPI LINAC are described in Reference [9]. The neutron energy at low energies which are assumed non-relativistic energy is given by

$$E_i = \frac{72.296L}{t_i - (t_0 - t_g)} \quad (1)$$

where E_i is the neutron energy in eV, L is the flight-path in m and t_i is the arrival time of the neutron and $(t_0 - t_g)$ is the time when the electron pulse impinges on the

target. t_0 is obtained by measuring the time gamma flash is detected. t_g is the flight time of gamma rays from the neutron target to the detector.

The capture yield Y_i in TOF channel i was calculated by

$$Y_i = \frac{C_i - B_i}{K\phi_{sm,i}}, \quad (2)$$

where C_i is dead-time-corrected and monitor-normalized counting rate of the sample measurement, B_i is dead-time-corrected and monitor-normalized background counting rate, K is product of the flux normalization factor and the detector efficiency $\phi_{sm,i}$ is smoothed, background-subtracted, and monitor-normalized neutron flux. The incident neutron flux shape was determined by mounting a 2.54-mm-thick, 97.9 wt % enriched $^{10}\text{B}_4\text{C}$ sample.

3. Data Analysis and results

Resonance parameters, neutron width Γ_n , radiation width Γ_γ , and resonance energy E_0 , were extracted from the Dy capture and transmission data sets using the SAMMY multilevel R-matrix Bayesian code [1]. Dy resonance parameters and spins from the ENDF/B-VII.1 evaluation [10] were used as the initial parameters in the energy region between 10 eV to 1 keV. The fitting was performed in order of transmission of natural Dy, capture yield of Dy isotope, and capture yield of natural Dy. When no further improvements in the fit were apparent, and the resonance parameters remained unchanged relative to the previous iteration, the parameters were deemed final. The SAMMY code was then used to calculate capture yield curves based on these final resonance parameters to compare with the experimental data from each Dy sample. We also examined each resonance listed in ENDF/B-VII.1 to check whether it was observed in the present data. If it did not look like a resonance peak, we removed the resonance from the parameter file.

We observed 7, 42, and 22 new resonances not listed in ENDF/B-VII.1 from ^{160}Dy , ^{161}Dy , and ^{163}Dy isotopes, respectively. Six resonances from ^{161}Dy isotope, two resonances from ^{163}Dy , and four resonances from ^{164}Dy listed in ENDF/B-VII.1 were not observed because the present measurements did not support their existence.

4. Statistical Analysis and Conclusion

The missing level curves of each isotope were plotted by assuming the level spacing is theoretically a constant. The average level spacing, D_0 , is the inverse of the slope in the range judged that D_0 is constant. The D_0 for ^{161}Dy and ^{163}Dy were judged to be constant up to 120.6 and 163.9 eV, respectively. It was assumed that the D_0 of ^{162}Dy and ^{164}Dy is constant up to 1000 eV because they have few resonances. The results were compared with the values from Reference 11 as shown in Figure 1.

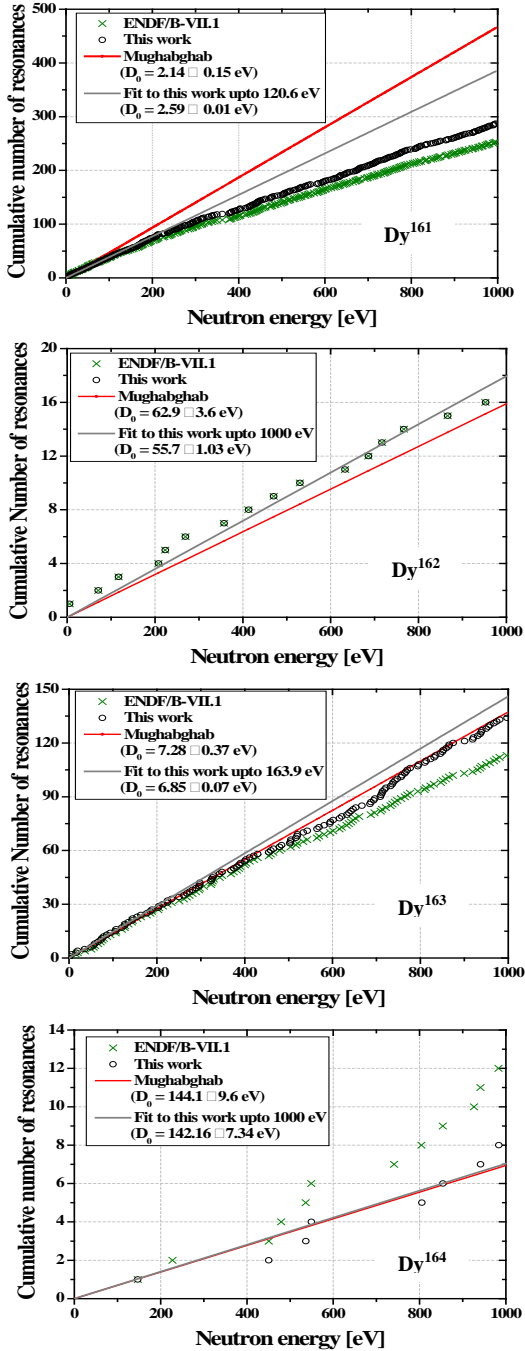


Figure 1. Staircase plot of level density for dysprosium isotopes.

Statistical distributions of reduced neutron were investigated for the three isotopes in the region from 0 to 1000 eV; ^{161}Dy , ^{162}Dy , and ^{163}Dy , but not for ^{164}Dy because of a few number of resonances. The reduced neutron widths Γ_n^0 were divided by the unweighted average reduced neutron width $\langle \Gamma_n^0 \rangle$ for each isotope. A cumulative distribution of these unitless ratios is compared with the integral of the Porter-Thomas distribution [12] (χ^2 distribution with one degree of freedom). The results agree reasonably with the Porter Thomas distributions. However, there are more narrow resonances than expected for ^{161}Dy and ^{163}Dy . These trends are also shown for ENDF/B-VII.1.

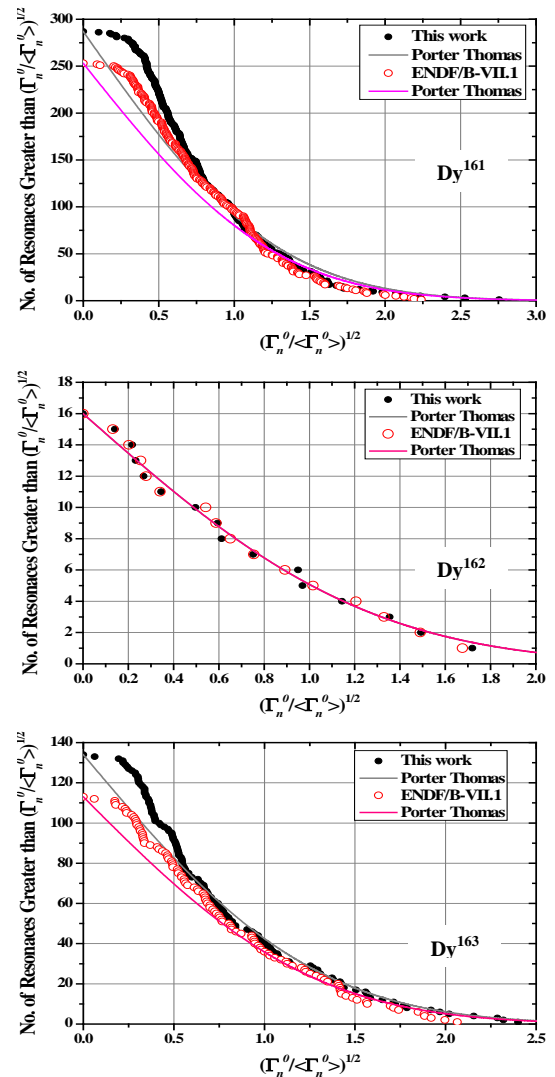


Figure 2. Cumulative reduced neutron width for the present measurements and ENDF/B-VII compared to Porter Thomas distribution.

Neutron strength functions, S_0 , were measured for the two isotopes with the most resonances, ^{161}Dy and ^{163}Dy . The values are compared with those of ENDF/B-VII.1 and the Atlas of Neutron Resonances [11] in the Table 1.

The S_0 were determined from the resonances within the energy range which was judged that the level density is constant. The uncertainties given in Table 1 were determined by a quadrature sum of the SAMMY-propagated uncertainties. S_0 for both ^{161}Dy and ^{163}Dy are larger than those from ENDF/B-VII.1 because most of resonances in this region are slightly stronger than suggested by ENDF. Otherwise, the values are smaller than those from Atlas.

Table 1. Neutron strength function S_0 for ^{161}Dy and ^{163}Dy .

	S_0 of ^{161}Dy [$10^{-4} \times \text{meV}^{-1/2}$]	S_0 of ^{163}Dy [$10^{-4} \times \text{meV}^{-1/2}$]
This work	1.67 ± 0.01	1.88 ± 0.02
ENDF/B-VII.1	1.58	1.61
Atlas of Neutron Resonances	1.82 ± 0.11	1.9 ± 0.2

Acknowledgment

This R&D was supported by BK21+ program through the National Research Foundation of Korea funded by the Ministry of Education and The National R&D Program through the Dong-nam Institute of Radiological & Medical Sciences (DIRAMS) funded by the Ministry of Science, ICT & Future Planning(50496-2016).

REFERENCES

[1] N. M. Larson, Updated Users Guide for SAMMY: Multilevel R-matrix fits to Neutron Data using Bayes equations, report ORNL/TM-9179/R8 (2008)

[2] Y. R. Kang et al., "Neutron Capture Measurements and Resonance Analysis of Dysprosium," Nuclear Data Sheets, **119**, p. 162 (2014)

[3] S. G. Shin et al., "Neutron Resonance Parameters of Dysprosium Isotopes Using Neutron Capture Yields," Proc. Korean Nuclear Society Autumn Meeting, Gyeongju, Korea, Oct 29-30 (2015)

[4] R. W. Hockenbury et al., "Neutron Radiative Capture in Na, Al, Fe, and Ni from 1 to 200 keV," Phy. Rev., **178**, 4, 1746 (1969)

[5] M. E. Overberg et al., "Photoneutron Target Development for the RPI Linear Accelerator," Nucl. Instrum. Meth. A., **438**, 253 (1999)

[6] R. E. Slovacek et al., "Neutron Cross-Section Measurements at the Rensselaer LINAC," Proc. Topl. Mtg. Advances in Reactor Physics, April 11–15, 1994, Knoxville, Tennessee, **2**, p. 193, American Nuclear Society (1994)

[7] N. J. Drindak et al., "A Multiplicity Detector for Accurate Low-Energy Neutron Capture Measurements,"

Proc. Int. Conf. Nuclear Data for Science and Technology, May 30–June 3, 1998, Mito, Japan, p. 383 (1998)

[8] R. C. Block et al., "Neutron Time-of-Flight Measurements at the Rensselaer LINAC," Proc. Int. Conf. Nuclear Data for Science and Technology, Gatlinburg, Tennessee, May 9–13, 1994, **1**, p. 81, American Nuclear Society (1994)

[9] G. Leinweber et al., "Resonance Parameters and Uncertainties Derived from Epithermal Neutron Capture and Transmission Measurements of Natural Molybdenum," Nucl. Sci. Eng. **164**, 287 (2010)

[10] M. B. CHADWICK et al., "ENDF/B-VII.1 nuclear data for science and technology: Cross sections, covariances, fission product yields and decay data," Nucl. Data Sheets, **112(12)**, 2887 (2011)

[11] S. F. Mughabghab, "Atlas of Neutron Resonances," fifth ed. Elsevier, New York (2006)

[12] C. E. Porter and R. G. Thomas, "Fluctuations of Nuclear Reaction Widths," Phys. Rev., **104**, **483** (1956)